

Thermodynamic evidence for the Bose glass transition in twinned $\text{YBa}_2\text{Cu}_3\text{O}_{7-\delta}$ crystals

D.J. Pérez-Morelo,¹ E. Osquiguil,¹ A. B. Kolton,² G. Nieva,¹ I. W. Jung,³ D. López,³ and H. Pastoriza¹

¹*Laboratorio de Bajas Temperaturas, Centro Atómico Bariloche and Instituto Balseiro, Comisión Nacional de Energía Atómica, Av. Bustillo 9500, R8402AGP S. C. de Bariloche, Argentina*

²*Teoría de la Materia Condensada, Centro Atómico Bariloche and Instituto Balseiro, Comisión Nacional de Energía Atómica, Av. Bustillo 9500, R8402AGP S. C. de Bariloche, Argentina*

³*Center for Nanoscale Materials, Argonne National Laboratory, Argonne, IL 60439, USA*

(Dated: March 24, 2022)

We used a micromechanical torsional oscillator to measure the magnetic response of a twinned $\text{YBa}_2\text{Cu}_3\text{O}_{7-\delta}$ single crystal disk near the Bose glass transition. We observe an anomaly in the temperature dependence of the magnetization consistent with the appearance of a magnetic shielding perpendicular to the correlated pinning of the twin boundaries. This effect is related to the thermodynamic transition from the vortex liquid phase to a Bose glass state.

PACS numbers: 74.25.Uv, 74.72.-h, 74.25.Bt, 74.25.-q

I. INTRODUCTION

The magnetic field - temperature phase diagram of vortex matter in high temperature superconductors exhibits a variety of thermodynamic phases and phase transitions whose properties are strongly influenced by the nature of the structural defects in the superconductors.¹ Particularly interesting is the case of spatially correlated defects, like twin boundaries and columnar tracks generated by heavy ion irradiation, because they produce correlated pinning on the vortex ensemble and can induce a new thermodynamic state called Bose glass.² This Bose glass phase is characterized by the collective alignment of the vortices into the correlated defects and has two distinctive characteristics: a vanishing of the linear electrical resistivity and a diverging elastic tilt modulus.³ As a result of this vortex localization, the Bose-glass phase will exhibit a transverse Meissner effect³: a finite transverse critical magnetic field is required to tilt the vortex lines away from the correlated defects. For magnetic fields larger than this critical transverse field, the vortex system acquires a tilted pinning state⁴ where vortices are partially locked along the correlated defects. In this state, usually identified as the staircase configuration, the capability to shield perpendicular magnetic fields is considerably reduced. The transition from the high temperature liquid state to the Bose glass phase will only occur when the angle between the external magnetic field and the correlated defects is small enough. Theory predicts that the angular dependence of the Bose glass critical temperature has a sharp maximum when the vortices are perfectly aligned with the correlated defects.³

Many experiments to test this phase transition have been performed in different superconductors with correlated defects and can be classified in two groups: transport measurements^{5,6} and shielding current measurements.^{7,8} From the first group of experiments clear evidence for the transition to a Bose glass state has been obtained through the scaling of the voltage versus

current data and the angular dependence of the critical temperature. Although these measurements show critical scaling its thermodynamic properties are hindered because of the out of equilibrium nature of the experiments. On the other hand, magnetic measurements⁹ have shown evidence for an enhancement of the shielding capability to perpendicular magnetic fields, but again these experiments were done far from equilibrium and can not discard that the observed effects were due to some metastable configuration.⁹ In this paper we used a micromechanical torsional oscillator to study the Bose glass transition in a micron size twinned $\text{YBa}_2\text{Cu}_3\text{O}_{7-\delta}$ crystal. Our results provide direct evidence of the transverse Meissner effect characteristic of this phase.

II. EXPERIMENTAL DETAILS

In this work we use a micromechanical oscillator device similar to the one used by Chan *et al.*¹⁰ and Decca *et al.*^{11,12} to obtain precise measurements of the Casimir force. Micromechanical oscillators have been used as magnetometers for microscopic magnetic and superconducting samples¹³ due to their high sensitivity,¹⁴ fast response and good performance at very high magnetic fields.¹⁵ Our device was fabricated using the multiuser process PolyMUMPs from the commercial foundry Memscap.¹⁶ It consists of a polysilicon paddle of $500 \times 500 \times 3.5\mu\text{m}^3$ anchored to the substrate by two $200\mu\text{m}$ long parallel rods of section $2 \times 2\mu\text{m}^2$ on each extreme. The torsional elastic constant for this design is $k = 5.41 \times 10^{-9}\text{Nmrad}^{-1}$. Two symmetric electrodes placed on the substrate underneath each flap allows the capacitive detection of the oscillator displacement. In Figure 1a we show a Scanning Electron Microscope picture of the device.

A circular $\text{YBa}_2\text{Cu}_3\text{O}_{7-\delta}$ (YBCO) single crystal with oriented twin boundaries is placed on top of the micromechanical oscillator (Figure 1a). The circular disk was

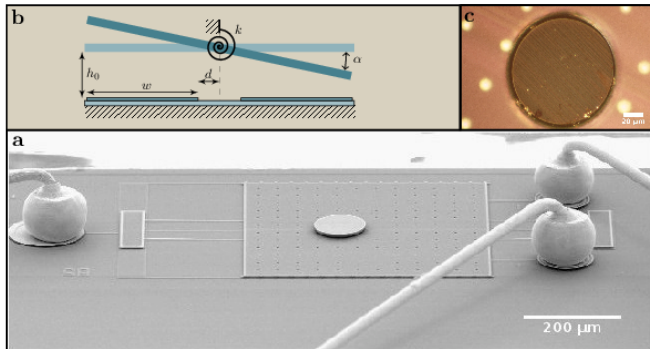


FIG. 1. a) Scanning Electron Microscope image of the Polysilicon mechanical torsional oscillator with the superconducting $\text{YBa}_2\text{Cu}_3\text{O}_{7-\delta}$ (YBCO) sample mounted on it. b) Cross section of the micro-mechanical Silicon Oscillator with the indication of the relevant geometrical dimensions. c) Polarized light microscopy picture of the measured disk glued to the oscillator. The normal of the twin planes were at 75 degrees from the rotational axis of the paddle.

carved out from a larger single crystal using a Focused Ion Beam milling tool. The disk final dimensions are $10\mu\text{m}$ of thickness and a diameter of $100\mu\text{m}$. The sample was glued to the micromechanical oscillator with a sub-micron drop of Apiezon N[®] vacuum grease using glass micro-pipettes and hydraulic manipulators under an optical microscope. Ultrasonic bonding was used to wire bond $25\mu\text{m}$ gold wires to connect the oscillator to a sapphire substrate which was later mounted in a rotatable holder of a Oxford Teslatron[®] variable temperature insert. The rotational axis of the holder is perpendicular to the uniform magnetic field generated by a superconducting magnet.

All data shown in this work were taken by sweeping temperature while keeping constant the angle θ_H between the magnetic field, \vec{H} , and the substrate. The experiments were performed using a field cooling protocol, e.g., the data were taken while lowering the temperature after applying the magnetic field at temperatures higher than the critical one. When the sample become superconducting, a magnetic torque,

$$\tau = \vec{M} \times \vec{H} \quad (1)$$

appears in the sample and the torsional plate of the micromechanical oscillator will rotate around its torsional axis.¹¹ This rotation is counteracted by the restoring torque caused by the deformation of the springs causing the plate to reach a tilt angle $\alpha = \tau/k$, where k is the oscillator's torsional spring constant.¹¹ In our experiment, the tilt angle α was obtained by measuring, with an Andeen-Hagerling AH 2700A bridge, the capacitance between the oscillator paddle and each of the electrodes symmetrically placed underneath. This capacitance is

modeled by the expression

$$C_{1,2} = \frac{\epsilon_0 L}{\tan(\pm\alpha)} \ln \left(\frac{h_0 + (d+w) \tan(\pm\alpha)}{h_0 + d \tan(\pm\alpha)} \right),$$

where L is the paddle length, h_0 is the distance between the oscillator and the electrodes at rest, d and w are the distances that describe the electrode geometry, and the $+, -$ signs correspond to the electrodes 1 or 2 respectively (see Figure 1b). Each angular value we report was obtained from the average of the measurements from both electrodes.

III. RESULTS

In Figure 2 we plot the oscillator angular response as a function of temperature for an applied magnetic field $\mu_0 H = 1\text{ T}$ oriented at different angles close to the c -axis direction. We observe several features in the data: first, for all measured angles the oscillator starts to deflect at 91.8 K coincident with the superconducting critical temperature of the YBCO. The deflection is symmetric for angles, θ_H , around the c -axis, and its magnitude increases as θ_H increases (in agreement with equation 1). This indicates that the micro-oscillator behaves essentially as a very sensitive magnetometer. Since the elastic constant of the torsional spring of our oscillator is temperature and field independent, for a fixed magnetization direction the deflection angle is proportional to the sample magnetization. The orientation of the magnetization for a given sample is the result of two competing energies. The Zeeman energy, minimized when the magnetization and the external magnetic field are parallel, and an anisotropy energy (taking into account the geometry and structure of the sample) minimized when the magnetization is aligned to an easy axis. For high temperature superconducting samples, due its anisotropy and plate-like shape, the direction of the reversible magnetization of the YBCO disk is almost parallel to the c -axis.¹⁷ Therefore our measurements in the high temperature range detect the magnitude of the c -axis magnetization.

In Figure 3a) we plot the calculated values for the disk magnetization as a function of temperature for different magnetic fields overlaying the data from Welp *et al.*¹⁸

For a small range of angles around the c -axis direction we observe a clear change of the behavior: At an angular and field dependent temperature, T^* , the tilt angle of the micromechanical oscillator reaches a maximum indicating that the magnetic torque exerted by the sample starts to diminish on further lowering the temperature (see Figure 2b). This behavior represents a sudden change in the temperature derivative of the magnetization, $\frac{dM}{dT}$, which is a thermodynamic signature for a second order phase transition.¹⁹

A simple explanation for the measured behaviour can be given in terms of the Bose glass model. At high temperatures, where the vortex ensemble is in the liquid state, the sample magnetization mainly points along

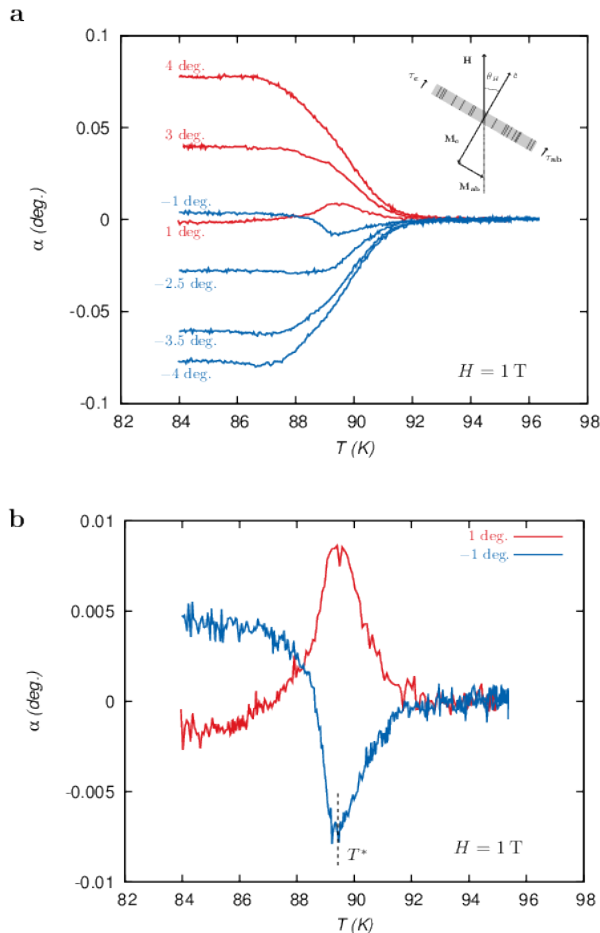


FIG. 2. a) Angular displacement of the Silicon torsional oscillator, α , as a function of temperature with an applied external magnetic field of 1T for different orientations, θ_H , between the substrate and the magnetic field. All data are taken from field cooling experiments, and show reversibility upon warming. For angles $|\theta_H| < 1.5$ deg the curves become non monotonic presenting a maximal value at a given temperature. The inset sketch a vectorial representation of the sample magnetization indicating the different angles involved in this experiment. In part b) we plot representative data for small θ_H showing the symmetric response around the c-axis direction.

the c-axis of the crystals due to sample geometry and material anisotropy. This magnetization exerts a “negative” torque on the sample-oscillator system. As soon as the sample enters into the Bose glass phase a transverse Meissner effect appears. The appearance of this effect implies that the sample magnetization has an extra component that is ≈ 90 degrees away from the c-axis. Such magnetization component counteracts the torque generated by the c-axis magnetization as is schematically shown in the inset of Figure 2a. This behavior is what our micromechanical magnetometer is reflecting, a reduction of the total torque exerted by the sample.

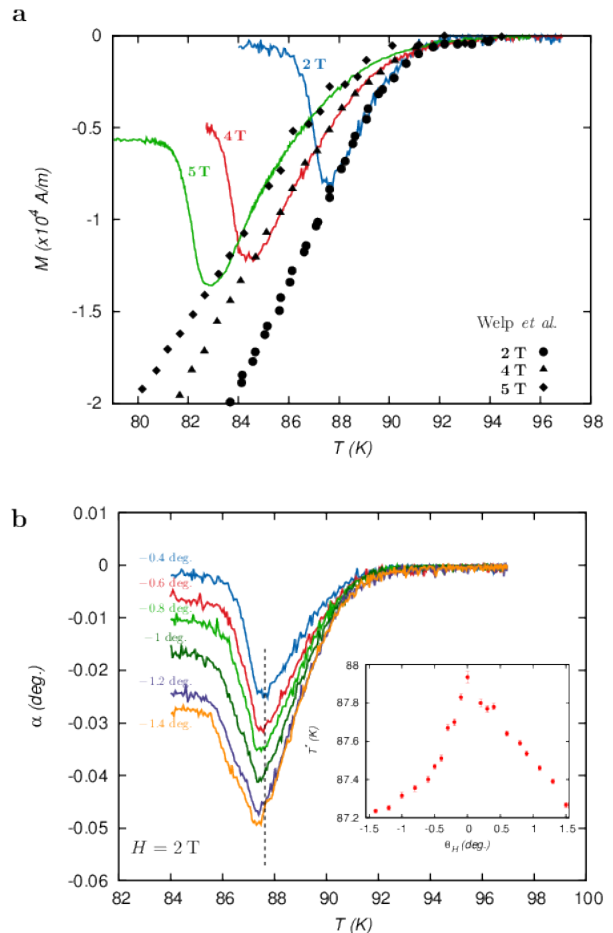


FIG. 3. a) Magnetization of the superconducting YBCO disk as a function of temperature for different applied magnetic fields. Continuous lines data obtained from our experiments and discrete points values extracted from Welp *et al.*¹⁸ b) Angular displacements of the oscillator as a function of temperatures for an applied field of 2T for values of θ_H close to zero. A clear shift to lower values for T^* as $|\theta_H|$ increases is visible. The inset plot the dependence of T^* as a function of the orientation, θ_H , for an applied magnetic field of 2T.

Further evidence that this observed anomaly is related to the Bose glass transition can be obtained by plotting T^* as a function of the sample angle, θ_H , shown in the inset of Figure 3b, for an applied field of 2T. The cusp-like shape of the transition temperature predicted for this phase transition is very clear. The data at this particular field shows an asymmetry between negative and positive angles. We can rule out that this effect is due to an experimental artifact like a magnetic field or temperature gradient at the sample position, an asymmetric response of the oscillator, or a thermal decoupling between the thermometer and the sample. One possibility for this asymmetric condensation energy of the Bose glass phase is a non uniformity at the samples edges. In micron sized samples like the reported here there is a significant frac-

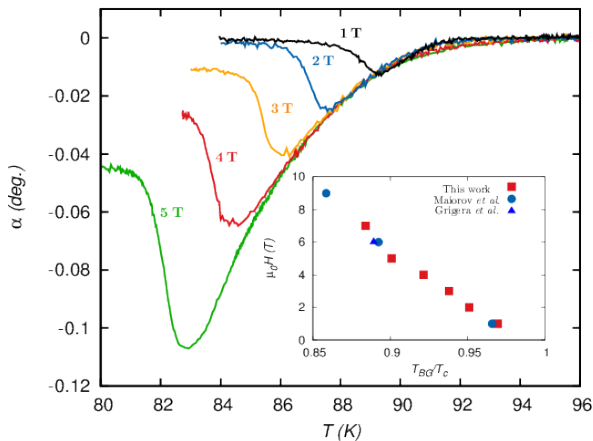


FIG. 4. a) Displacement angle of the oscillator as a function of temperature for different magnetic fields applied at an angle $\theta_H = -0.4$ deg. Inset: Magnetic field versus Temperature phase diagram for the measured dM/dT discontinuity in comparison with Bose glass critical temperatures obtained from transport measurements reported by Grigera *et al.*,⁶ and Maiorov *et al.*⁵

tion of vortices that are affected by surface effects. We must also remark that in a previous work⁵ was observed a change in the T_{BG} vs θ dependence as a function of the applied magnetic field. At low fields a linear dependence was reported and at high fields a sharper cusp-like functionality was found. In our case we are measuring both dependences at the same applied magnetic field but at negative or positives angles.

In the inset of Figure 4 we summarize the position of the measured anomaly in a H-T phase diagram. For comparison, data obtained from the scaling of transport measurements^{5,6} for similar crystals are plot in the same graph, showing a perfect agreement with our data.

Figure 4 shows representative data taken at the same

nominal θ_H at different magnetic fields. A clear field dependence for the $\frac{dM}{dT}$ discontinuity is observable. Moreover, the curves for all fields merge for temperatures above this feature indicating that the magnetization has a close to $1/H$ dependence in the reversible vortex liquid state. At temperatures closer to the critical one this data overlap is lost, indicating that a different scaling functionality must be taken into account. In this temperature range 3D thermal fluctuations on the thermodynamic magnetization were observed.²⁰

IV. CONCLUSIONS

In summary we have presented experimental evidence of the thermodynamic nature of the vortex system Bose glass transition in high quality $\text{YBa}_2\text{Cu}_3\text{O}_{7-\delta}$ single crystals. The temperature and angular dependences of the magnetic response, measured by a high sensitive Silicon micro oscillator is fully consistent with a continuous transition at T_{BG} and correspond to the appearance of a spontaneous magnetic shielding to the perpendicular component of the magnetic field.

ACKNOWLEDGMENTS

DJPM Fellowship holder of Consejo Nacional de Investigaciones Científicas y Técnicas (CONICET). EO ABK, GN and HP researchers of CONICET. This work was partially supported by PIP 1122008010111001, CONICET. This work was performed, in part, at the Center for Nanoscale Materials, a U.S. Department of Energy, Office of Science, Office of Basic Energy Sciences User Facility under Contract No. DE-AC02-06CH11357. We thank V. Bekeris for a careful reading of the manuscript and valuable suggestions.

¹ G. Blatter, M. V. Feigel'man, V. B. Geshkenbein, A. I. Larkin, and V. M. Vinokur, "Vortices in high-temperature superconductors," *Rev. Mod. Phys.* **66**, 1125–1388 (1994).
² David R. Nelson and V. M. Vinokur, "Boson localization and pinning by correlated disorder in high-temperature superconductors," *Phys. Rev. Lett.* **68**, 2398–2401 (1992).
³ D. R. Nelson and V. M. Vinokur, "Boson localization and correlated pinning of superconducting vortex arrays," *Phys. Rev. B* **48**, 13060 (1993).
⁴ E. B. Sonin, "Pinning of vortices by parallel twin boundaries in superconducting single crystals," *Phys. Rev. B* **48**, 10487–10497 (1993).
⁵ B. Maiorov and E. Osquiguil, "Vortex solid state in $\text{YBa}_2\text{Cu}_3\text{O}_{7-\delta}$ twinned crystals," *Phys. Rev. B* **64**, 052511 (2001).
⁶ S. A. Grigera, E. Morr e, E. Osquiguil, C. Balseiro, G. Nieva, and F. de la Cruz, "Bose-glass phase in twinned $\text{YBa}_2\text{Cu}_3\text{O}_{7-\delta}$," *Phys. Rev. Lett.* **81**, 2348–2351 (1998).

⁷ A. W. Smith, H. M. Jaeger, T. F. Rosenbaum, W. K. Kwok, and G. W. Crabtree, "Bose glass melting and the transverse Meissner effect in $\text{YBa}_2\text{Cu}_3\text{O}_{7-\delta}$ single crystals," *Phys. Rev. B* **63**, 064514 ((2001)).
⁸ A. A. Zhukov, G. K. Perkins, J. V. Thomas, A. D. Caplin, H. K pfer, and T. Wolf, "Direct observation of tilted vortex structures induced by twin boundaries in $\text{YBa}_2\text{Cu}_3\text{O}_y$ single crystals," *Phys. Rev. B* **56**, 3481 ((1997)).
⁹ A. W. Smith, H. M. Jaeger, T. F. Rosenbaum, A. M. Petrean, W. K. Kwok, and G. W. Crabtree, "Vortex flow and transverse flux screening at the Bose glass transition," *Phys. Rev. Lett.* **84**, 4974 ((2000)).
¹⁰ H. B. Chan, V. A. Aksyuk, R. N. Kleiman, D. J. Bishop, and F. Capasso, "Quantum mechanical actuation of microelectromechanical systems by the Casimir force." *Science* **291**, 1941 (2001).
¹¹ R. S. Decca, D. Lopez, E. Fischbach, and D. E. Krause, "Measurement of the Casimir force between dissimilar met-

- als,” *Phys. Rev. Lett.* **91**, 050402 (2003).
- ¹² Francesco Intravaia, Stephan Koev, Il Woong Jung, A. Alec Talin, Paul S. Davids, Ricardo S. Decca, Vladimir A. Aksyuk, Diego A. R. Dalvit, and Daniel López, “Strong Casimir force reduction through metallic surface nanostructuring,” *Nature Commun.* **4** (2013).
- ¹³ C. A. Bolle, V. Aksyuk, F. Pardo, P. L. Gammel, E. Zeldov, E. Bucher, R. Boie, D. J. Bishop, and D. R. Nelson, “Observation of mesoscopic vortex physics using micromechanical oscillators,” *Nature* **399**, 43 ((1999)).
- ¹⁴ M. I. Dolz, W. Bast, D. Antonio, H. Pastoriza, J. Curiale, R. D. Sánchez, and A. G. Leyva, “Magnetic behavior of single $\text{La}_{0.67}\text{Ca}_{0.33}\text{MnO}_3$ nanotubes: Surface and shape effects,” *J. Appl. Phys.* **103**, 083909 (2008).
- ¹⁵ V. Aksyuk, F. F. Balakirev, G. S. Boebinger, P. L. Gammel, R. C. Haddon, and D. J. Bishop, “Micromechanical “trampoline” magnetometers for use in large pulsed magnetic fields,” *Science* **280**, 720–722 (1998).
- ¹⁶ MEMSCAP Inc., 4021 Stirrup Creek Drive, Durham, NC 27703, USA.
- ¹⁷ Ernst Helmut Brandt, “Superconductor disks and cylinders in an axial magnetic field. I. Flux penetration and magnetization curves,” *Phys. Rev. B* **58**, 6506–6522 (1998).
- ¹⁸ U. Welp, W. K. Kwok, G. W. Crabtree, K. G. Vandervoort, and J. Z. Liu, “Magnetic measurements of the upper critical field of $\text{YBa}_2\text{Cu}_3\text{O}_{7-\delta}$ single crystals,” *Phys. Rev. Lett.* **62**, 1908–1911 (1989).
- ¹⁹ Onuttom Narayan and A. P. Young, “Free energies in the presence of electric and magnetic fields,” *American Journal of Physics* **73**, 293–298 (2005).
- ²⁰ U. Welp, S. Fleshler, W. K. Kwok, R. A. Klemm, V. M. Vinokur, J. Downey, B. Veal, and G. W. Crabtree, “High-field scaling behavior of thermodynamic and transport quantities of $\text{YBa}_2\text{Cu}_3\text{O}_{7-\delta}$ near the superconducting transition,” *Phys. Rev. Lett.* **67**, 3180–3183 (1991).